Geographic Divergence in Population Genomics and Shell Morphology Reveal History of Glacial Refugia in a Coastal Dogwhelk

Emily K. Longman[1], Joaquin C.B. Nunez[1], Eric Sanford[2,3], & Melissa Pespeni[1]

[1] Department of Biology, University of Vermont, Burlington, VT, USA

[2] Bodega Marine Laboratory, University of California Davis, Bodega Bay, CA, USA

[3] Department of Evolution and Ecology, University of California Davis, Davis, CA, USA

Corresponding Author: Emily K. Longman, Emily.Longman@uvm.edu

Keywords: *Nucella canaliculata*, Population genomics, Geometric morphometrics, Phylogeography, Ecological genomics

Abstract:

Studying contemporaneous spatial patterns of genomic diversity can yield important insights into the evolutionary processes that structure populations and shape patterns of adaptation. In contrast to the large number of marine species with planktonic larvae, populations of marine taxa with low dispersal and deep evolutionary divergences offer an opportunity to reveal the phylogeographic histories of marine ecosystems. Here, we constructed a draft genome assembly for the low-dispersing marine dogwhelk, *Nucella canaliculata*, and studied patterns of genomic diversity and shell morphometrics in 19 populations distributed along ~1,500 km of the west coast of North America. We observed significant population structure with a strong phylogeographic break at Monterey Bay, which was matched with divergence in shell morphology. Genomic patterns, concomitant with computer simulations, suggest that there were at least two refugial populations during the last glacial maximum that subsequently experienced post-glacial expansion and admixture. Lastly, linking genotype to phenotype, we identified candidate loci underlying variation in shell morphology. These findings demonstrate how high-resolution genomic data reveal the roles of demography, selection, and historical events in shaping the spatial distribution of genetic variation, offering key insights into the processes that structure modern coastal populations and their potential to respond to future climatic changes.

31 **Introduction:**

32 Understanding the population structure and demography of a species is essential for
33 interpreting patterns of adaptation and linking phenotypic variation to its genetic bases [1].
34 Spatially and temporally varying selection pressures [2], historical events [3,4], biogeographic
35 barriers to dispersal [5], and life history patterns [6], can all shape the present-day geographic
36 distribution of populations and the genetic diversity they harbor. However, our understanding of
37 population structure and subsequently the molecular bases of adaptation in many species is
38 significantly hindered by the lack of genomic resources for non-model organisms [7,8]. This
39 demographic information is of pressing concern because an understanding of extant levels of
40 genomic diversity is needed to predict a species' adaptive capacity and vulnerability to a rapidly
41 changing climate [9].

42 In marine ecosystems, understanding population connectivity and genetic diversity is
43 further complicated by extrinsic factors such as oceanographic processes [10-13], as well as
44 intrinsic factors including the wide range of life history strategies and developmental modes
45 present in marine organisms [6]. The location of phylogeographic breaks and the level of
46 population structure often reflect a species' reproductive strategy and dispersal potential; species
47 with direct development have low dispersal potential and typically have much more defined
48 genetic structure than species with planktonic larvae [11,14,15]. Further, as a result of the low
49 levels of gene flow in taxa with direct development there is an increased probability that
50 historical separation among populations persists for many generations [11,16,17]. Thus, patterns
51 of genetic diversity of species with low dispersal often represent deeper evolutionary divergence
52 over longer timescales than species with high dispersal potential [16–18]. Therefore, studying the
53 phylogeographic structure of low-dispersing species lends insight into the processes shaping the

54 evolutionary history of marine ecosystems and potential responses to rapid global change during
55 the modern era [16]. However, low dispersing species also have a greater likelihood of adapting
56 to strong selective forces, possibly complicating observed patterns of genetic diversity [19].
57 Fossil assemblages of calcifying marine species along the northeast Pacific coast from the
58 late Pleistocene show that the geographic distribution of many species shifted equatorially in
59 response to Pleistocene climatic fluctuations [20,21]. Classic genetic models of Pleistocene
60 glaciation suggest that these climatic changes should impact present-day genetic diversity, with
61 greater genetic diversity in areas of glacial refugia than areas of population expansion, and high
62 dissimilarity between refugial populations due to the deeper divergence time [3,4]. Several
63 genetic studies show evidence of effects of glacial refugia, particularly those on low dispersing
64 taxa suggesting phylogeographic breaks at Monterey Bay and the long stretches of sandy
65 beaches around Los Angeles, California [11,16,22]. Studies using coalescent approaches with
66 mitochondrial markers and agnostic nuclear loci in co-distributed species along the northeastern
67 Pacific have revealed strong phylogeographic breaks that reflect both Pleistocene glaciation and
68 patterns of connectivity, genetic drift, and natural selection [15,23,24]. Recent advances in
69 generating and analyzing genome-wide genetic diversity data, particularly when applied in low
70 dispersal species, can provide greater resolution of these demographic patterns and the role of
71 geological events in shaping patterns of present-day genetic diversity [25,26]. For example,
72 whole genome sequencing of the kelp species *Alaria esculenta* indicates that high-latitude glacial
73 refugia in the North Atlantic persisted through cycles of glaciation [26]. In addition, such high-
74 resolution data can be used to reveal the genetic bases of complex phenotypic traits and to test
75 for signatures of natural selection against the neutral, genome-wide genomic background, while
76 controlling for demography [1,27].

The channeled dogwhelk, *Nucella canaliculata*, is a promising study system to investigate phylogeographic patterns of divergence. This dogwhelk is a species of predatory gastropod (Family Muricidae) that lives on rocky shores from central California to Alaska and consumes mussel and barnacle prey via a chemo-mechanical mode of feeding [28–30]. Females lay benthic egg capsules, and crawl-away young establish in the surrounding area, thus the species has low dispersal potential [29,31]. Additionally, individuals reside only in mussel beds on wave-exposed headlands, thus populations are isolated due to intervening sandy beaches. Previous research has revealed patterns of local adaptation with striking spatial variation in predatory drilling ability [32–34], foraging behavior [35], and heat tolerance [36]. Despite the wealth of ecological knowledge about *N. canaliculata*, there is a lack of genomic resources for the species, limiting our understanding of the molecular mechanisms generating these adaptive patterns. Genetic studies of the mitochondrial locus cytochrome oxidase I (*mtCOI*) suggest that populations display a pattern of isolation by distance and that the southern-most sampled population in central California was the most genetically diverged [30]. In accord, previous work using allozymes and mtDNA on *Nucella* congeners suggest strong population structure along the Pacific coast and northward range expansion post Pleistocene glaciation [23,24]. For example, genetic diversity of *N. emarginata* is greatest near the southern end of the species' distribution [23], and population divergence times of *N. lamellosa* indicate that northern populations probably re-colonized post last glacial maximum [24]. Thus, the biogeographic patterns of intraspecific trait variation and the habitat specificity of *N. canaliculata* suggest that the population genomics of this low dispersing taxa may reveal spatially complex phylogeographic patterns.

99 Here, we present a high-quality draft genome assembly generated from a single *Nucella*
100 *canaliculata* individual, a genome-wide panel of genetic variation from 19 populations spanning
101 ~1,500km of the west coast of North America using pooled-sequencing [37], and analyses of
102 shell morphometrics from dogwhelks collected across the 19 field sites. There is a long history of
103 malacologists using geographic variation in shell morphology as an indicator of potential
104 isolation and genetic divergence among gastropod populations [16,38,39]. Thus, our analyses
105 explore whether spatial variation in morphological traits is concordant with the phylogeographic
106 patterns revealed by the genomic data. Additionally, we integrate the genomic and
107 morphological data to begin to link genetic and phenotypic variation. Specifically with these
108 genomic and morphological datasets, we aimed to address the following questions: 1) How is
109 genetic diversity in *N. canaliculata* spatially structured along ~1,500km of the west coast of
110 North America? 2) Do patterns of genetic diversity appear to be structured more strongly by
111 contemporary or historical processes? 3) Does variation in shell morphology suggest a similar
112 biogeographic pattern of divergence as the genomic data? 4) Lastly, what are the molecular bases
113 for intraspecific variation in shell morphology? Overall, our analyses revealed strong population
114 structure with congruence between genomic and phenotypic datasets, as well as evidence of
115 glacial refugia.
116
117 **Methods:**
118 ***Genome Sequencing and Assembly***
119 Genome assembly was based on source DNA extracted from one adult female dogwhelk
120 collected from Bodega Marine Reserve, California (38°19’8”, -123°4’28”) in June 2022. High
121 molecular weight DNA extraction from flash frozen foot tissue, library preparation and

122 sequencing (Oxford Nanopore PromethION and Element Bio AVITI 600 flow cell) occurred at
123 the DNA Technologies and Expression Analysis Core at the UC Davis Genome Center (see
124 Appendix S1: Section S1 for more details).

125 We assembled the genome using a hybrid assembly approach using `DBG2OLC` [40]. This
126 approach combines the continuity of the Oxford Nanopore long reads and the quality of the
127 AVITI short reads (see Appendix S1: Section S1 for more details). Genome quality and
128 completeness was quantified using `QUAST` [41] and `BUSCO` [v5.7.1] [42]. Repeats and low
129 complexity DNA sequences were masked using `RepeatMasker` [v4.1.6] with the model
130 trained on the Pacific oyster, *Crassostrea gigas* [43]. Genome annotation of the softmasked
131 genome occurred using `Augustus` [v3.5.0] trained on *Drosophila melanogaster* [44].

132 ***Field Collections, DNA Extractions and SNP Calling***

133 We collected 20 adult (>18 mm in length) *N. canaliculata* from 19 populations ($N = 380$)
134 along the Pacific coast of North America (Table S1). Collections occurred during low tide at the
135 19 rocky headlands from October 2023 to July 2024. Directly after field collections, we sampled
136 and preserved in 95% EtOH foot muscle tissue for each dogwhelk. We extracted the DNA from
137 each individual dogwhelk using an E.Z.N.A Mollusc & Insect DNA Kit (Omega Bio-Tek,
138 Norcross, Georgia) with minor modifications. For each extraction, we determined DNA quality
139 and quantity using gel electrophoresis, a Nanodrop, and a Qubit. Then, for each population,
140 DNA from the 20 individuals was pooled in equimolar amount. Subsequent library preparation
141 (Watchmaker DNA library preparation kit [Watchmaker Genomics, Boulder, Colorado] with 6
142 PCR cycles) and sequencing (150 base pair paired-end sequencing on two lanes of NovaSeqX
143 25B) was performed at the DNA Technologies and Expression Analysis Core at the UC Davis
144 Genome Center.

We trimmed the low-quality pooled sequences with `fastp` [v0.23.4] [45], then mapped the reads to the softmasked *N. canaliculata* reference genome using `bwa-mem2` [v2.2.1] [46]. We filtered, sorted and removed duplicate reads from the binary alignment map (bam) files, then merged the bam files from the two sequencing lanes. Mean coverage of the bam files was 33.13, with an average mapping rate of 57.25 (Table S2). We hypothesize that the low mapping rate is due to the genome containing many repetitive regions, a common problem of Molluscan genomes [47], and the short-read sequences being unable to map to these highly repetitive regions. We used `freebayes` [v1.3.6] to call variants from the 19 bam files [48] and subsequently performed stringent filtering of the VCF file with `vcftools` [v0.1.16] and the `poolfstat` R package [49] (Appendix S1: Section S2).

Population Structure and Genomic Diversity

Population structure was analyzed using principal component analysis (PCA) and F_{ST}. The VCF file was converted to a pooldata object using the *vcf2pooldata* function in the `poolfstat` R package [49]. A PCA was performed using the *randomallele* function. We calculated a global F_{ST} metric, a block-jackknife estimation of F_{ST}, and a multi-locus F_{ST} over a sliding window of 1kb using the *computeFST* function. Additionally, we estimated pairwise-population F_{ST} using the *compute.pairwiseFST* function using the ANOVA method. Lastly, population demography was characterized by analyzing the **Ω** matrix in `BayPass` [v2.41] [50].

We tested for isolation by distance by evaluating whether there was a relationship between pairwise genetic distance, $F_{ST}/(1- F_{ST})$, and geographic distance. Given that *N. canaliculata* lacks a planktonic larval stage, distance between sites was measured as the distance along the coastline using the measure tool on Google Maps. We used Mantel tests (1,000 permutations) to determine the significance of the relationships using the `ecodist` R package.

168 We calculated nucleotide diversity (π), Watterson's estimator (θ), and Tajima's D for
169 each population using `npstat` [v1] [51]. To do so, the bam file for each population was
170 converted to pileup format, then calculations for each statistic were performed on a 25kb sliding
171 window with a minimum and maximum coverage of 20 and 120, respectively, a minimum base
172 quality of 30 and a minimum allele count of 5.

173 ***Demographic Inference and Population Genetic Simulations***

174 Our population genetic analyses revealed distinct patterns of genetic structure and π in
175 the samples nearest Monterey Bay (i.e., PL, SBR, and PGP), consistent with signatures of post-
176 glacial secondary encounter. We used a two-pronged approach to study these genetic patterns.
177 First, to investigate the patterns of population structure, we tested two models of post-glacial
178 demography using the coalescent framework implemented in `moments` [v1.2.2] [52] on folded
179 site frequency spectra fit to Pool-Seq data using a pipeline similar to that described in [53]. We
180 asked whether the PL, SBR, and PGP samples are the product of a population expansion from a
181 single southern glacial refugium (i.e., A→B→C), or, alternatively, if they are the product of a
182 secondary encounter between two glacial refugia (i.e., A→B←C). For the latter scenario we
183 explicitly modeled the admixture proportions between the hypothetical admixed refugia. For
184 each model we report the Akaike Information Criterion (AIC) across 10 optimization runs, each
185 initiated from randomly sampled starting parameters (Appendix S1: Section S3). To translate
186 coalescent units into chronological time, we scaled the output of the model (i.e., θ) by the factor
187 $4L\mu$; where L is the length of sequence and μ is the mutation rate of *Drosophila melanogaster*
188 $2.8\text{x}10^{-9}$ [54].

189 To further investigate whether the patterns of π at PL, SBR, and PGP can be explained by
190 either the single expansion model, or the two-refugia model, we conducted forward genetic

simulations using `SLiM` [v5.0] [55]. Unlike our `moments` analysis, which used *N. canaliculata* data, the goal of these forward simulations was to contextualize the patterns of genetic variation expected under two proposed scenarios. These scenarios were generally similar in demographic structure to the models tested using `moments`, however, our SLiM simulations consisted of seven demes arranged in a stepping-stone fashion, representing latitudinally distributed populations (Appendix S1: Section S3). The models tested were: 1) a one-refugium model where the first deme recolonizes the entire habitat after an extinction event, and 2) a two-refugia model, where the habitat is recolonized by demes 1 and 7 post an extinction event. For both models, we quantified simulated nucleotide diversity (π) and compared the spatial pattern to the empirical data.

Dogwhelk Shell Geometric Morphometrics

Shell morphology was characterized using landmark analysis. We took photographs of the ventral surfaces of the 380 field-collected *N. canaliculata* from the 19 populations using a Canon DSLR camera with a Canon EF 28-136mm f/3.5-5.6 IS lens on a tripod. We utilized `tpsUtil` (v1.83) and `tpsDig` (v2.31) to place 15 landmarks on predefined locations on the ventral surface of the shell [56]. Dogwhelks with damaged shells were removed from the analyses ($N = 10$). We analyzed the data used the `geomorph` R package [57] and the program `MorphoJ` [58]. We performed a Procrustes transformation to remove variation in dogwhelk orientation using the *gpagen* function then analyzed the Procrustes coordinates using PCA. We also tested for intraspecific variation in shell shape as a function of size (quantified as the log of the centroid size for each dogwhelk), site or latitude, and their interaction with a Procrustes ANOVA using the *procD.lm* function with 1,000 permutations.

Detection of the Genomic Bases of Morphological Variation

We identified outliers associated with shell morphology using `BayPass` [v2.41] [50]. The coefficient of variation for PC1 and PC2 of the morphological data were used as phenotypic input data for `BayPass`. Outlier SNPs were identified using a Bonferroni threshold (alpha = 0.05/8,277,206 = 6.04×10^{-9}), then subsequently annotated with `SnpEff` [59]. Putative functional annotation of proteins was done using `blast` against Molluscan taxa within the UniProtKB reference proteomes – Swiss-Prot database.

Results:

The First Draft Genome of Nucella canaliculata

We utilized a hybrid assembly approach using a combination of Oxford Nanopore Technologies PromethION long reads and Element Bio AVITI short reads to generate the first genome of *Nucella canaliculata*. The *de novo* assembly was very large (total assembly length of 1.57 Gb) and consisted of numerous scaffolds (Table 1). BUSCO scores indicate that the draft genome was 91.0% and 80.7% complete for Eukaryota and Mollusca, respectively (Table 1; Table S3).

Table 1. *Nucella canaliculata* genome assembly and quality metrics. Eukaryota BUSCO scores (n = 255).

Assembly Length (bp)	1,571,681,309
Number of Contigs/Scaffolds (bp)	18,944
Largest Contig/Scaffold (bp)	2,196,136
GC %	42.52%
N50 (bp)	146,860
L50 (bp)	3,117
Complete BUSCOs (Single Copy; Duplicated)	91.0% (85.1%; 5.9%)
Fragmented BUSCOs	4.7%
Missing BUSCOs	4.3%

Patterns of Population Structure

The Pool-Seq data were used to analyze patterns of spatial population structure and genomic diversity. After stringent filtering, our final SNP list for the 19 pools contained 8,277,206 SNPs. The principal component analysis (PCA) showed strong clustering of populations based on geography (Figure 1A; Figure S1). PC1 captured 30.54% of the variation and strongly partitioned the populations into two clusters, one north and one south of Monterey Bay. PC2 to PC5 all further subdivided the seven populations in the southern cluster. It was not until PC6 (4.79% of the variance) that there was notable separation among the 12 populations in the cluster north of Monterey Bay.

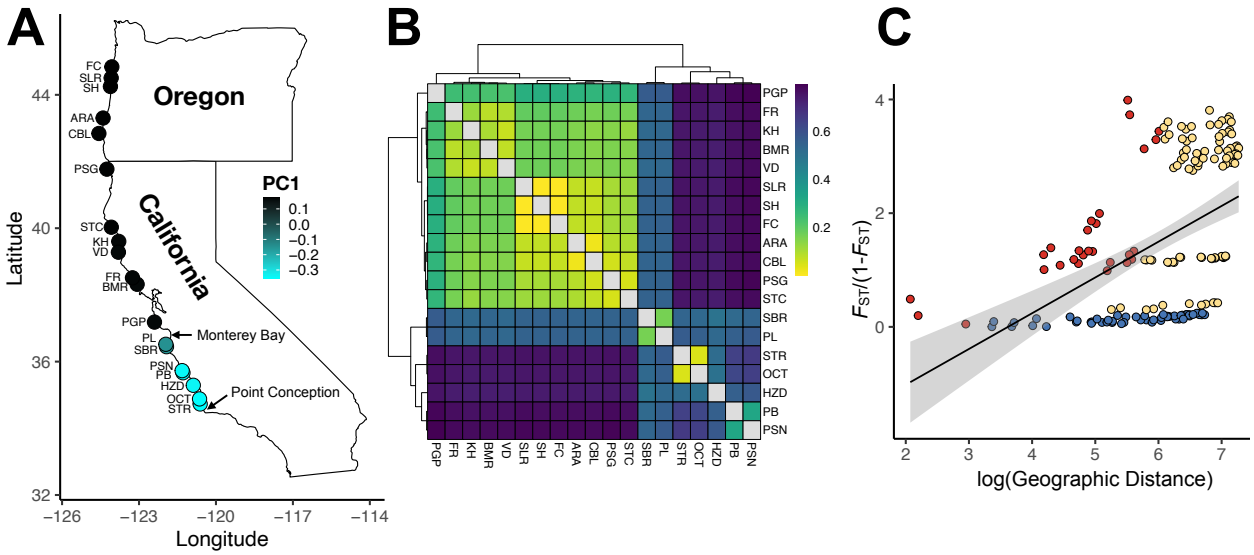

Figure 1. Population structure and genetic variation among the 19 *Nucella canaliculata* populations along the coast of California and Oregon, USA. A) Projections of the first principal component analysis (PCA) loadings on the map of the collection sites. The map shows the site codes and other biogeographically relevant landmarks. B) Heatmap of pairwise F_{ST} for the 19 populations. Blue and yellow indicate high and low levels of genetic differentiation, respectively. C) The log of the geographic distance in km between sites and genetic distance. Color indicates which sites are being compared — both in the southern cluster (red), both in the northern cluster (blue), and a comparison between a northern and southern site (yellow). See Table S1 for an explanation of the population codes and coordinates.

The genome wide global F_{ST} was 0.582 (Table S4). Multi-locus F_{ST} indicated high levels of F_{ST} distributed evenly across the genome (Figure S2). Pair-wise F_{ST} among the 19 populations

255 ranged from 0.002 to 0.8 (Table S5). The greatest differentiation occurred between populations
256 south versus north of Monterey Bay (top right corner of Figure 1B). There was little genetic
257 differentiation among the populations north of Monterey Bay. In contrast, there was highly
258 variable amounts of genetic differentiation among the populations south of Monterey Bay
259 (bottom right corner of Figure 1B). Hierarchical clustering based on the `BayPass` population
260 covariance matrix recapitulated the clustering of the populations into two genetically distinct
261 groups (Figure S3).

262 Across the 19 populations, *Nucella canaliculata* displayed a pattern of isolation by
263 distance (Mantel test for all 19 populations, $R^2 = 0.480$, P-value = 0.001; Figure 1C). However,
264 this pattern was only present when contrasting populations across the southern versus northern
265 genetic cluster, and within the southern cluster. Despite their greater geographic distance, there
266 was no pattern of isolation by distance among the populations north of Monterey Bay (blue dots
267 in Figure 1C).

268 All 19 populations had very low levels of genetic variation, heterozygosity and Tajima's
269 D (Figure 2; Figure S4; Table S6). The two populations just south of Monterey Bay, SBR and
270 PL, had the highest heterozygosity and nucleotide diversity (Figure 2). Despite mean nucleotide
271 diversity being similar across most of the populations (Table S6), the distribution and median
272 nucleotide diversity strongly differed by geography (Figure 2B). The majority of populations
273 south of Monterey Bay had a broader range of nucleotide diversity and low median π, while the
274 populations north of Monterey Bay had a very narrow range of nucleotide diversity and higher
275 median π. Almost all populations, except the three populations closest to Monterey Bay (SBR,
276 PL and PGP) had negative median Tajima's D values indicating an excess of rare alleles in each
277 population (Figure 2C; Table S6). The 11 most northern populations had mean Tajima's D

values that were more negative than the five most southern populations. This pattern is indicative of an excess of rare alleles in the northern populations and is consistent with recent population expansion.

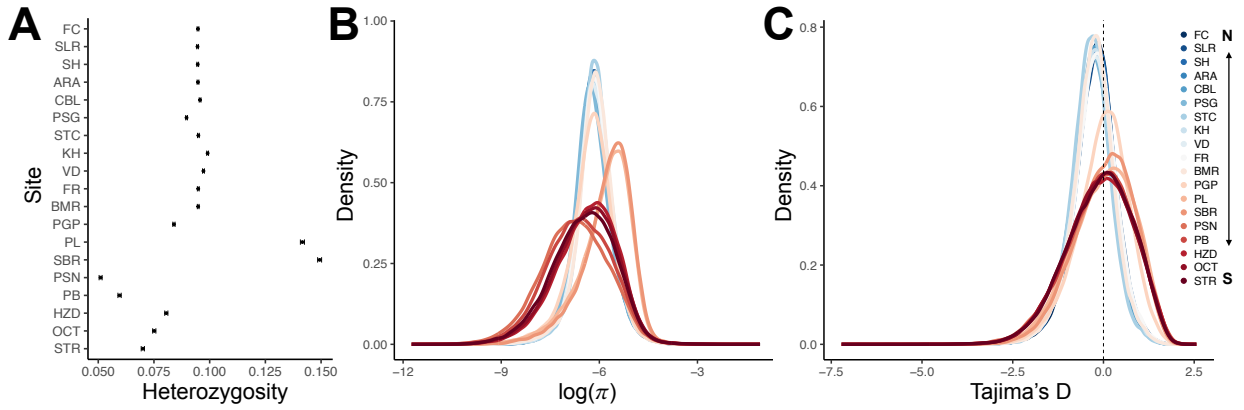

Figure 2. A) Within-population block-jackknife estimate ± standard error of heterozygosity for the 19 *N. canaliculata* populations from `poolfstat`. Populations are ordered north to south from top to bottom. B) Nucleotide diversity ($Log_{10}(\pi)$), and C) Tajima's D across the 19 populations. Calculations were performed on a sliding window with a 25kb window size. The dashed vertical line for Tajima's D indicates 0, the expected value under a neutral model. The colors indicate the 19 populations.

Genomic Evidence of Post-Glacial Demography

The patterns of genetic variation observed in populations near Monterey Bay (see Figure 2; i.e., PGP, PL, and SBR) suggest that these mid-latitude populations may have originated from a secondary contact between hypothetical northern and southern refugia. To evaluate this hypothesis, we performed coalescent demographic inference with `moments` [52] to compare whether the patterns of genetic variation at the sites nearest Monterey Bay matched either of two phylogeographic models: (1) a single southern refugium expanding northward, or (2) a secondary contact (admixture) between two, formerly allopatric, glacial refugia. Our results indicate that, for all three populations, the admixture model provides a better fit based on AIC values (Figure 3A; Figure S5 for results with less stringent SNP filtering, demonstrating the robustness of the pattern to SNP calling methods). The ΔAIC (Log_{10} transformed) values for the

300 admixture model, relative to the expansion model, were: PGP = 5.40; PL = 6.62; and SBR =

301 6.83.

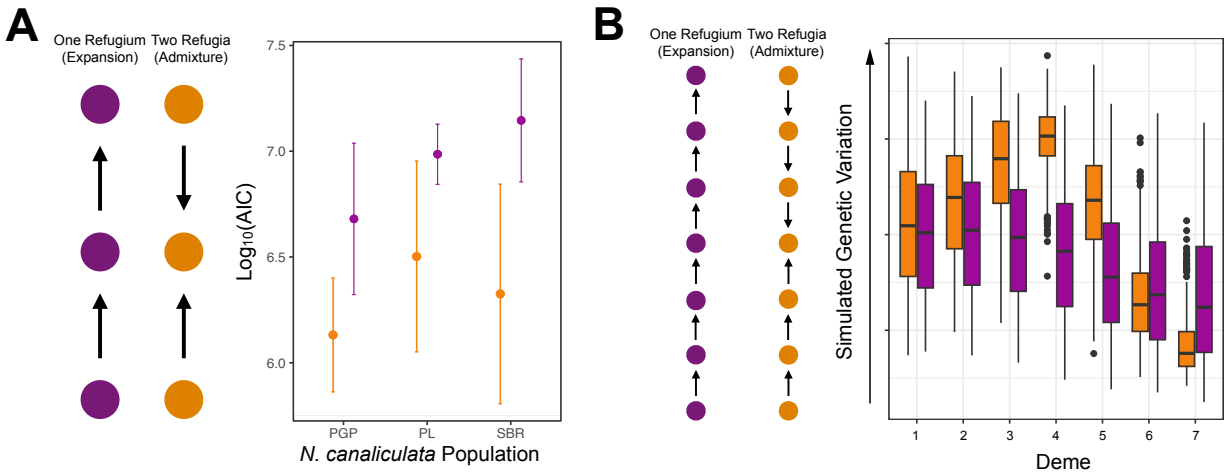

302

303 **Figure 3.** A) Distribution of AIC values for the two demographic models tested using `moments`
304 for the three *N. canaliculata* populations nearest Monterey Bay. The mean ± standard deviation of
305 AIC for the 10 model replicates is shown (the best model is reported in the text). B) Hypothetical
306 levels of genetic variation derived from simulating the two proposed demographic scenarios using
307 `SLiM`.
308

309 For PGP, the best-fitting model supported an admixture scenario, albeit with very low

310 southern ancestry contribution (~1%), indicating that most of its genetic ancestry derives from

311 northern populations (Figure 3A). This aligns with its position as the southern boundary of the

312 northern genetic cluster (Figure 1A). In contrast, PL and SBR exhibit strong signatures of

313 admixture between northern and southern populations, with southern admixture contributions of

314 57% and 59% for PL and SBR, respectively. These admixture events are roughly estimated to

315 have occurred approximately 7,000-10,000 years ago. However, these estimates remain uncertain

316 because the mutation rate for *Nucella* is not characterized. Nevertheless, these results suggest

317 that PL and SBR are situated at the "core" of the admixture zone between the hypothetical

318 northern and southern glacial refugia.

319 Our analyses indicate the presence of an admixture zone, suggesting at least one ancestral
320 cluster located to the north and to the south of Monterey Bay. To further evaluate these patterns,
321 we implemented forward-time genetic simulations in `SLiM` [55], enabling comparison of
322 observed genetic variation with simulated expectations. Among the simulated models, the "two
323 refugia" scenario produced patterns of genetic variation most consistent with our empirical data
324 (Figure 3B). In this model, deme 4, the hypothetical mid-latitude "admixture core", exhibited the
325 highest levels of genetic variation. Additionally, in this simulation, genetic variation decreased
326 monotonically away from the admixture zone at a rate proportional to the simulated population
327 size of each refugium (the second refugium, present at deme 7, had a smaller population size
328 relative to the first refugium, present at deme 1). In contrast, the one refugium model produced a
329 different pattern, in which genetic variation steadily declined with range expansion, lacking the
330 pronounced peaks in diversity seen in the admixed populations in the two-refugia model and in
331 the real data.
332
333 ***Shell Geometric Morphometrics Show Patterns of Spatial Differentiation***
334 Given the strong signature of genetic divergence among populations, we explored
335 whether shell morphology displayed a similar pattern of divergence by performing landmark
336 analysis (Figure 4A). PC1 (21.60% of the variance) and PC2 (19.65%) explained most of the
337 shape variation and geographically separated the populations based on shell shape (Figure 4B;
338 Figure S6). PC1 described a shell shape with a lack of elongation of the spire and a rotundness of
339 the main body whorl and aperture (wireframe image for PC1 on Figure 4B). PC2 described shape
340 changes in the widest point of the outer lip and the angle of the siphonal canal. Dogwhelks from
341 populations south of Monterey Bay occupy a greater amount of PC space than the northern

dogwhelks despite there being fewer populations analyzed. When comparing pairwise Procrustes distances, the greatest divergence in shape was between the populations south of Monterey Bay with those from northern California and southern Oregon (dark blue/teal section in the top right of Figure 4C). However, it is notable that one population south of Monterey Bay, HZD, clustered with the Oregon populations. Size (measured as centroid size) and population explained 5.5% and 21.6% of the dogwhelk shape variation (Table S8). Similarly, size, latitude and their interaction all explained a significant amount of the variance in dogwhelk shape (Figure S6D; Table S8).

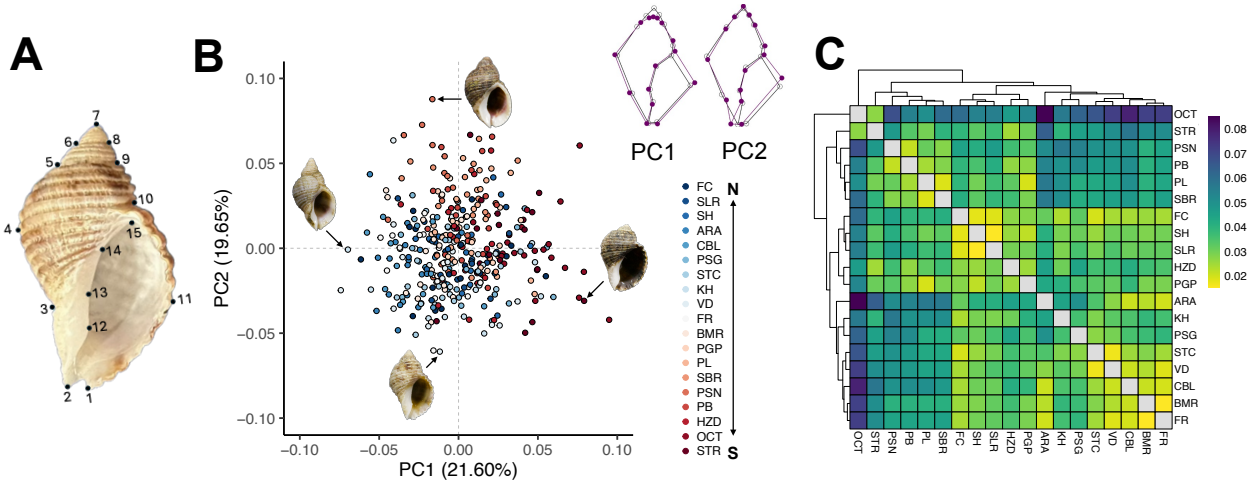

Figure 4. Results of geometric morphometric comparisons of *N. canaliculata* shells from 19 populations. A) Diagram showing the position of the 15 landmarks. B) Principal component 1 and 2 of the Procrustes coordinates. Dogwhelks are colored by population. The shells of 4 *N. canaliculata* are highlighted to represent the shape variation quantified for each PC. Wireframes display the shape variation for each PC (purple) in relation to the mean shape (black). C) Heatmap of Procrustes distances among the 19 populations. See Table S1 for an explanation of population codes.

A Shell Matrix Protein Emerges as a Genomic Outlier of Local Adaptation

We used `BayPass` to identify outlier SNPs associated with morphological variation. Seven Bonferroni corrected outlier SNPs were identified associated with the coefficient of variation for PC1 (Figure 5A), and six outlier SNPs were identified associated with the

coefficient of variation for PC2 (Figure 5B). Four candidate loci were in the same protein (gene *g26813*), with one SNP (position 41601) identified in both analyses (Table S9). Most of the populations south of Monterey Bay were fixed at these four loci, while the populations north of Monterey Bay were polymorphic with variable allele frequencies (Figure 5C). Three of the loci show strong associations with morphology — when the allele frequency approaches 0 the morphometric space becomes negative (Figure S7). To identify the function of this protein of interest, we ran `blastp`. This protein has been identified as a shell matrix protein in multiple mollusc species including the zebra mussel, *Dreissena polymorpha* (UniProt entry: A0A9D4NEM1; percent identity 26.2%, positive matches = 52.4%, E-value = 0.0002) [60], and the lettuce slug, *Elysia crispata* (UniProt entry: A0AAE1DT89; percent identity 24.3%, positive matches = 45.0%, E-value = 0.00044) [61].

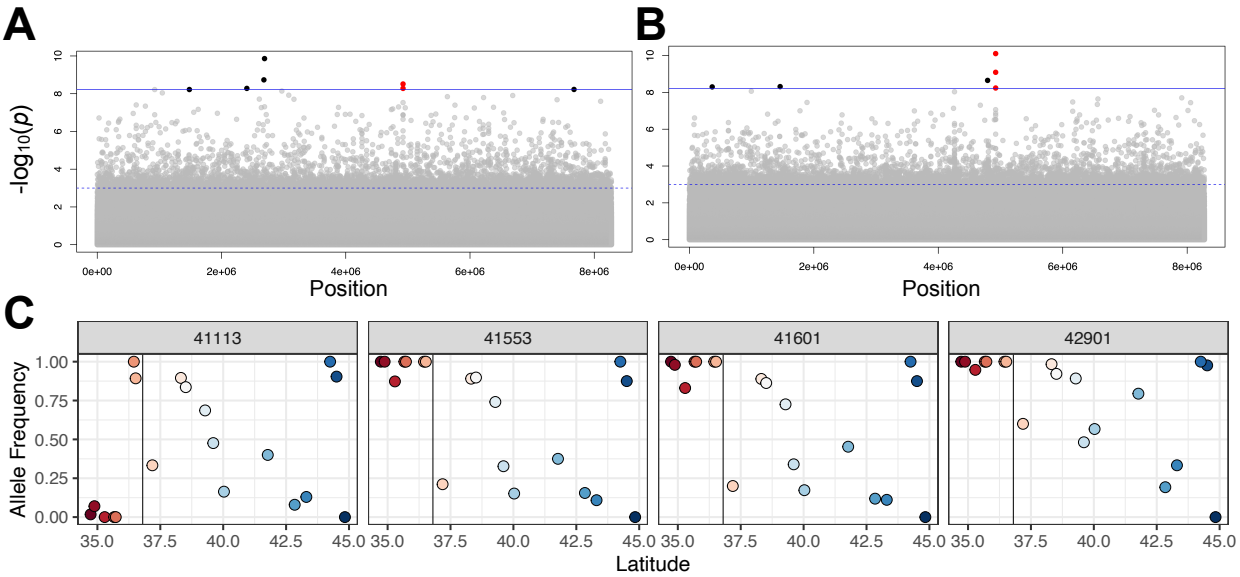

Figure 5. Signatures of selection from `BayPass` for the coefficient of variation A) for PC1 and B) for PC2 of the *N. canaliculata* shell morphology. The solid blue line indicates Bonferroni corrected outliers and the dotted blue line indicates significance of SNPs at a value of 0.001. Bonferroni corrected outliers are identified in black, with the four candidate loci on gene *g26813* in red. C) Allele frequencies of the four candidate loci on gene *g26813* as a function of latitude. The solid black line indicates the location of Monterey Bay.

382 **Discussion:**

383 The present-day genomic diversity and population structure of a species reflects a
384 combination of contemporary and historical processes [5]. In contrast to most marine species
385 which have high population connectivity due to planktonic larvae, the genomics of marine taxa
386 with direct development and low dispersal provide an especially powerful opportunity to analyze
387 deeper evolutionary histories and the impacts of historical events [16–18]. Our pooled
388 sequencing of 19 populations of the low-dispersing channeled dogwhelk, *Nucella canaliculata*,
389 across ~1,500 km of the west coast of North America indicated a high level of population
390 structure, with a phylogeographic split at Monterey Bay, and a pattern of genomic diversity that
391 revealed a history of being structured by past geological events. The contemporary genomic
392 patterns and accompanying computer simulations suggest that during the last glacial maximum
393 there were at least two refugial populations, north and south of Monterey Bay, that experienced
394 post-glacial expansions and admixture. This biogeographic pattern of divergence was further
395 supported by spatial variation in shell morphology. Additionally, we identified putatively
396 adaptive outlier loci that may be the molecular drivers of variation in shell morphology. Our
397 findings have important management implications; if the range of this species shifts poleward, as
398 predicted with climate change, there is risk of losing the unique genetic diversity that is primarily
399 maintained in the populations near the species' southern range limit.

400 ***Phylogeography and Glacial Refugia***

401 Pleistocene glaciation drove changes in species distributions, with most temperate marine
402 species in the northern hemisphere retreating southward to escape glacial ice sheets [20,21].
403 Geological assemblages from Pleistocene terraces along the west coast of North America
404 indicate that many species, including *N. canaliculata*, shifted their ranges due to climatic

405 fluctuations in accord with shifting habitat conditions [20,21]. Genetic models suggest high
406 genetic diversity within areas of glacial refugia and high dissimilarity between refugial
407 populations, and low genetic diversity in the area of subsequent population expansion [3].
408 Previous work using coalescent-based methods with mitochondrial markers and several
409 anonymous nuclear loci found that Pleistocene glaciation left a signature on the current genetic
410 composition of populations of several marine species in the northeast Pacific [11,16,23,24]. In
411 particular, studies on low dispersing gastropod taxa with benthic development show genetic
412 signatures of northward range expansion post glaciation [16,23,24]. In contrast, the high
413 dispersal potential present in most marine species [6] and the importance of oceanographic
414 processes and vicariant barriers in structuring genetic diversity typically overwhelms any
415 remnant signature of Pleistocene glaciation [13,62]. However, advancements in SNP-based
416 approaches are increasing our phylogeographic resolution and power to detect the persistent
417 influence of glaciation [25,26].
418 Our genome-wide data revealed that the present-day phylogeographic structure of *N.*
419 *canaliculata* showed clear evidence of glacial refugia, followed by population expansion and
420 admixture (Figure 2; Figure 3). We revealed two genetically distinct clusters with Monterey Bay
421 being the phylogeographic breakpoint (Figure 1). All populations north of Monterey Bay were
422 genetically similar and have a negative Tajima's D value, indicating population expansion
423 (Figure 2C). In contrast, the populations between Monterey Bay and the species southern range
424 limit of Point Conception contained variable levels of nucleotide diversity and were highly
425 diverged from each other despite their spatial proximity (Figure 1; Figure 2). These patterns
426 closely match those predicted from genetic models of Pleistocene glaciation [3,7]. Additionally,
427 the populations nearest Monterey Bay show a unique signature of higher nucleotide diversity and

428 heterozygosity compared to the populations to the north and south, suggesting potential
429 admixture in this region (Figure 2).

430 Our `moments` analyses and `SLiM` simulation results provided greater clarity to this
431 glacial pattern as well as unique insights about the fine scale demography of the species,
432 particularly about the evolutionary histories of the populations nearest Monterey Bay. These
433 analyses suggest that at least one northern refugium persisted through the cycles of glaciation,
434 rather than the entire contemporary species being derived from southerly populations (Figure 3).
435 These refugial populations expanded post-glacially and experienced a secondary contact near
436 Monterey Bay. Further, the admixture proportions show that the two populations just south of
437 Monterey Bay (PL and SBR) are the 'true' admixed zone, while the region just north of
438 Monterey Bay (i.e., PGP) is the likely southern edge of the northern refugia. The drastic drop in
439 admixture proportions between PL and PGP, in the context of the F_{ST} findings (Figure 1),
440 suggests that admixture was relatively recent, and that migration is low.

441 While our demographic inference results provide promising insights into the species'
442 phylogeography, they should be interpreted with caution given the limitation of Pool-Seq data.
443 Because allele frequencies are inferred from read counts rather than individual genotypes, rare
444 variants are often underrepresented, biasing the site frequency spectrum toward common variants
445 [53,63]. This reduces sensitivity to recent bottlenecks, which are typically detected through
446 changes in rare allele abundance, and can lead to underestimation of their severity or timing.
447 Given this limitation, we did not attempt to model explicit glacial bottleneck scenarios; instead,
448 we focused on estimating admixture proportions in mid-latitude populations, since admixture
449 patterns are insensitive to assumptions about mutation rates and have been shown to yield
450 estimates comparable to those obtained from other approaches (e.g., compare [53] to [64]).

451 Lastly, several key genetic parameters for *Nucella* remain uncharacterized – thus, we relied on
452 published rates from the invertebrate model system *Drosophila*. Consequently, parameters
453 related to population divergence and admixture timing should be considered approximations and
454 interpreted with caution.

455 Genetic variation in the northern populations indicates that the phylogeographic history
456 of *N. canaliculata* may be more complex than suggested by our models of glacial refugia. Under
457 a simple scenario of a "large" southern refugia and a "small" (or remanent) northern refugia, we
458 should expect to see a peak in genetic variation at the region of admixture and a sharp decline in
459 the levels of standing genetic variation towards the northern edge (Figure 3B). Yet, in our data,
460 we see a peak in variation at SBR and PL, with variable variation in the southern populations and
461 stable levels of genetic variation in the northern populations that are, on average, higher than the
462 southern sites (Figure 2B). One possible hypothesis to explain this departure from expectations is
463 that the southern refugia was smaller than the northern refugia; this would be unusual, but not
464 impossible (see [4]). For example, strong competition with other snails in the southern refugia or
465 limitations in prey availability could have kept populations small [65]. An alternative hypothesis
466 could be that there were multiple northern refugia that experienced sequential mixing post-
467 glaciation, giving rise to the elevated variation. To clarify these patterns and determine the exact
468 location and size of the northern refugia, we would need more thorough sampling of populations
469 near the species northern range limit, or ancient samples.

470 Understanding the present-day phylogeographic structure of a species is particularly
471 important as natural populations are being forced to either rapidly adapt or shift their geographic
472 ranges in response to anthropogenic climate change [9]. Most of the unique genetic diversity of
473 *N. canaliculata* (i.e., suggested by high F_{ST}) was in the populations south of Monterey Bay.

474 Given that populations at the warmer, trailing edge of a range are more likely to go extinct in
475 response to climate change, this could mean losing large amounts of endemic diversity [17],
476 particularly for species with low dispersal. In accord, recent research that surveyed several
477 coastal marine species, including *N. canaliculata*, across their ranges in the northeast Pacific
478 found that populations near their equatorward edge are demographically vulnerable to climate
479 change and environmental stress [66]. Population density of *N. canaliculata* declined
480 latitudinally from Oregon to central California in association with increasing aerial and water
481 temperature stress, and a reduction in rocky habitat availability [66]. Small populations are
482 highly vulnerable to local extirpation due to Allee effects and stochastic events [67], and there is
483 accumulating evidence that marine heatwaves and other oceanic extreme events are becoming
484 increasingly common [68]. Thus, there is substantial risk that the genetically unique, but
485 demographically small, populations of *N. canaliculata* near their trailing edge could face local
486 extirpation.

487 ***Adaptive consequences of low dispersal potential***

488 The phylogeographic pattern of defined population structure and low levels of genetic
489 diversity that we observed has likely impacted the adaptive potential and evolutionary trajectory
490 of *N. canaliculata* populations. Previous research studying intraspecific variation in predatory
491 drilling ability in *N. canaliculata* showed that the species displays a pattern of local adaptation
492 [30,32–34]. However, rather than a smooth latitudinal gradient, the adaptive landscape appears to
493 be a spatial mosaic, with specific sites deviating from regional patterns [33,34]. Despite their
494 geographic separation, the populations with the greatest drilling ability are SBR and VD. Our
495 genomic results provide important demographic context to this phenotypic pattern and suggest
496 that these two populations have strikingly different genetic backgrounds, with SBR being an

497 admixed population and VD being in the northern genetic cluster. Thus, this phenotypic pattern
498 of parallel adaptation could be due to the populations evolving strong drilling using independent
499 molecular pathways either via the same or different morphological mechanism. This hypothesis
500 is further supported by the fact that these two populations display different behavioral patterns
501 when exposed to predator cues [35]. Research that links genotype to phenotype would be needed
502 to elucidate the molecular mechanisms behind this adaptive landscape.

503 For many species, linking phenotype to genotype and understanding patterns of
504 adaptation are significantly hindered by the lack of genomic resources for non-model organisms
505 [7,8]. The genome assembly presented here is the first for the species, and the second for the
506 ecologically important genus *Nucella* [69]. Extraction of high-quality molluscan DNA is a
507 challenge due to the presence of mucopolysaccharides and other secondary metabolites [70].
508 Additionally, molluscan genomes are large, have a high proportion of repetitive regions, and
509 typically harbor high heterozygosity, thus genome assembly is computationally difficult and
510 relatively few genomes have been assembled, despite there being more than 100,000 living
511 molluscs taxa [47]. Like previously published molluscan genomes [47,69], the *N. canaliculata*
512 assembly presented here was very large and consisted of numerous scaffolds. Despite this, the
513 assembly was smaller than the estimated genome size for the species of 2.54pg±0.057 [71], a
514 pattern not uncommon in molluscan genomes [47].

515 ***Shell Morphology and Species Taxonomy***

516 Given their ubiquity and longevity, the calcareous shells of gastropods have long been
517 used to infer taxonomy and evolutionary patterns [39,72]. Despite this, few modern
518 phylogeographic studies of marine gastropods incorporate morphological data alongside genetic
519 data (but see [16,38]). We found evidence that *N. canaliculata* dogwhelks show spatial variation

520 in shell morphology, with the greatest difference between populations south versus north of
521 Monterey Bay (Figure 4C), consistent with geographic patterns of genomic divergence.
522 Dogwhelks from southern populations were typically more rotund and had a shorter spire,
523 compared to dogwhelks from northern populations (Figure 4A). Additionally, the size of the
524 dogwhelks varied latitudinally with the largest dogwhelks present at SBR and PL (Figure 4B).
525 Shell morphology in *Nucella* is a result of both phenotypic plasticity [35] and adaptive evolution
526 [73]. Consequently, the morphometric data (Figure 4) showed a less stark pattern of divergence
527 among populations than the genomic data (Figure 1). Notwithstanding, the concordance of our
528 datasets increases our confidence in the biogeographic pattern. Further, this pattern mirrors
529 results from other gastropod taxa, which show evidence that Pleistocene range expansion
530 impacts the geographic distribution of variation in shell morphology [16,38]. For example, a
531 study of *N. ostrina* and *N. emarginata* suggests that range expansion post glaciation caused
532 secondary contact of the two species and subsequently the evolution of shell shape via character
533 displacement [38].

534 Our genomic and morphometric results both indicate a strong spatial signal of divergence
535 with a breakpoint at Monterey Bay. This biogeographic pattern in *N. canaliculata* matches an
536 overlooked taxonomic hypothesis, based on shell morphology, that there may be a northern and
537 southern subspecies divided at Monterey Bay [74]. In this context, what had previously been
538 hypothesized as two morphological subspecies, are according to our data, two
539 phylogeographically distinct genetic clusters that are readily able to breed [33], whose
540 morphological differences reflect divergent histories of demography and selection.

541 To test for signatures of selection and begin to link genotype to phenotype, we ran
542 `BayPass` on the coefficient of variation for PC1 and PC2 of the shell morphology dataset. This

543 framework allowed us to identify outlier loci while controlling for population structure. We
544 identified a handful of SNPs associated with both coefficients of variation (Figure 5). Notably,
545 one protein stood out in both analyses. The four candidate loci on this protein display a spatial
546 pattern such that most are fixed in the populations south of Monterey Bay and polymorphic in
547 the populations north of Monterey Bay (Figure 5C). This protein has been identified as a shell
548 matrix protein in other mollusc species, including the zebra mussel, *Dreissena polymorpha* [60],
549 and the lettuce slug, *Elysia crispata* [61]. Interestingly, *E. crispata* has secondarily lost its shell
550 as an adult, though it has a shell as a veliger, thus it retains shell matrix proteins [75]. We
551 hypothesize that this protein is likely a candidate for morphological variation and local
552 adaptation and should be studied further.
553 Overall, this research highlights the power of genomic approaches to advance our
554 understanding of how historical events have shaped contemporary demography in coastal
555 species. The geographic distribution of genomic diversity in *Nucella canaliculata* reveals a
556 persistent signature of glacial events in the northeast Pacific, with important implications for
557 adaptive capacity and conservation in an era of rapid global change.
558
559 **Data Accessibility Statement:**
560 The *Nucella canaliculata* genome assembly can be found at BioProject accession number
561 PRJNA1282036 and the raw reads for the assembly can be found under the BioProject accession
562 number PRJNA1282048
563 (https://dataview.ncbi.nlm.nih.gov/object/PRJNA1282048?reviewer=a33a83up9ei8j53qhvpc3j3s
564 3k). Raw pooled-sequencing reads can be found under the SRA BioProject accession number
565 PRJNA1276871

566 (https://dataview.ncbi.nlm.nih.gov/object/PRJNA1276871?reviewer=pv82mfjf2dfa7tihlf0caot03
567 5), and the individual BioSample accession numbers can be found in Table S1. A GitHub
568 repository with the code for analyzing the data can be found at https://github.com/emily-
569 longman/Nucella_can_Pop_Genomics.
570 **Ethics:** Collections in California were performed under CA Fish & Wildlife Scientific Collecting
571 Permits S-191200004-19122-001 and S-190980002-23226-001, and specific use amendments S-
572 190980003-23226-001-01 and S-190980003-23226-001-02, and CA State Parks permit 24-820-
573 015 and amendment 24-820-015A. Collections in Oregon were performed under the taking
574 permit 27976.
575 **Author's contributions:** E.K.L.: conceptualization, data curation, formal analysis, funding
576 acquisition, investigation, methodology, project administration, resources, software, supervision,
577 validation, visualization, writing – original draft, writing – review & editing; J.C.B.N.: formal
578 analysis, software, visualization, writing – review & editing; E.S.: funding acquisition,
579 investigation, writing – review & editing; M.P.: conceptualization, methodology, resources,
580 supervision, writing – review & editing. All authors gave final approval for publication and
581 agreed to be held accountable for the work performed therein.
582 **Funding:** This research was supported by an NSF postdoctoral fellowship (OCE-2307933)
583 awarded to E.K.L. and the National Science Foundation grant OCE-1851462 awarded to E.S.
584 **Acknowledgements:** We thank the Vandenberg Space Force Base, the UC Reserve System and
585 the Abbott family for access to field sites. We thank N. Longman and J. Fosnight for assistance
586 with the field collections, and R. A. Bay, B. B. Cameron, and E. S. Nielsen for help with
587 optimizing the extraction protocol and discussions about sequencing approaches for the genome.
588

589 **References:**

590 [1] Luikart, G., England, P., Tallmon, D., Jordan, S. & Taberlet, P. (2003). The power and
591 promise of population genomics: from genotyping to genome typing. *Nature Reviews*
592 *Genetics, 4,* 981-994. (https://doi.org/10.1038/nrg1226)

593 [2] Saccheri, I., & Hanski, I. (2006). Natural selection and population dynamics. *Trends in*
594 *Ecology & Evolution*, *21*(6), 341–347. (https://doi.org/10.1016/j.tree.2006.03.018)

595 [3] Hewitt, G.M. (1996). Some genetic consequences of ice ages, and their role in divergence
596 and speciation. *Biological journal of the Linnean Society*, *58*(3), 247–276.
597 (https://doi.org/10.1111/j.1095-8312.1996.tb01434.x)

598 [4] Maggs, C.A., Castilho, R., Foltz, D., Henzler, C., Jolly, M.T., Kelly, J., Olsen, J., Perez, K.E.,
599 Stam, W., Väinölä, R., et al. (2008). Evaluating signatures of glacial refugia for North
600 Atlantic benthic marine taxa. *Ecology, 89*(sp11), S108–S122. (https://doi.org/10.1890/08-
601 0257.1)

602 [5] Avise, J.C. (2000). *Phylogeography: the history and formation of species*. Harvard
603 University Press. (https://doi.org/10.2307/j.ctv1nzfgj7)

604 [6] Thorson, G. (1950). Reproductive and larval ecology of marine bottom invertebrates.
605 *Biological Reviews of the Cambridge Philosophical Society, 25*, 1–45.
606 (https://doi.org/10.1111/j.1469-185X.1950.tb00585.x)

607 [7] Savolainen, O., Lascoux, M., & Merilä, J. (2013). Ecological genomics of local
608 adaptation. *Nature Reviews Genetics*, *14*(11), 807–820. (https://doi.org/10.1038/nrg3522)

609 [8] Da Fonesca, R.R. Albrechtsen, A., Themudo, G.E., Ramos-Madrigal, J., Sibbesen, J.A.,
610 Maretty, L., Zepeda-Mendoza, M.L., Campos, P.F., Heller, R., & Pereira, R.J. (2016).

Next generation biology: sequencing and data analysis approaches for non-model organisms. *Marine genomics, 30*, 3–13. (https://doi.org/10.1016/j.margen.2016.04.012)

[9] Waldvogel, A.M., Feldmeyer, B., Rolshausen, G., Exposito-Alonso, M., Rellstab, C., Kofler, R., Mock, T., Schmid, K., Schmitt, I., Bataillon, T., et al. (2020). Evolutionary genomics can improve prediction of species' responses to climate change. *Evolution Letters*, *4*(1), 4–18. (https://doi.org/10.1002/evl3.154)

[10] Crawford, D.L., & Oleksiak, M.F. (2016). Ecological population genomics in the marine environment. *Briefings in Functional Genomics*, *15*(5), 342–351. (https://doi.org/10.1093/bfgp/elw008)

[11] Pelc, R.A., Warner, R.R., & Gaines, S.D. (2009). Geographical patterns of genetic structure in marine species with contrasting life histories. *Journal of Biogeography*, 36(10), 1881–1890. (https://doi.org/10.1111/j.1365-2699.2009.02138.x)

[12] Wares, J.P., Gaines, S.D., & Cunningham, C.W. (2001). A comparative study of asymmetric migration events across a marine biogeographic boundary. *Evolution, 55*(2), 295-306. (https://doi.org/10.1111/j.0014-3820.2001.tb01294.x)

[13] Kelly, R.P., & Palumbi, S.R. (2010). Genetic structure among 50 species of the northeastern Pacific rocky intertidal community. *PloS one*, *5*(1), e8594. (https://doi.org/10.1371/journal.pone.0008594)

[14] Riginos, C., Douglas, K.E., Jin, Y., Shanahan, D.F., & Treml, E.A. (2011). Effects of geography and life history traits on genetic differentiation in benthic marine fishes. *Ecography*, *34*(4), 566–575. (https://doi.org/10.1111/j.1600-0587.2010.06511.x)

[15] Dawson, M.N., Hay, C.G., Grosberg, R.K., & Raimondi, P.T. (2014). Dispersal potential and population genetic structure in the marine intertidal of the eastern North Pacific. *Ecological Monographs, 84*(3), 435-456. (https://doi.org/10.1890/13-0871.1)

[16] Hellberg, M.E., Balch, D.P., & Roy, K. (2001). Climate-driven range expansion and morphological evolution in a marine gastropod. *Science, 292*(5522), 1707–1710. (https://doi.org/10.1126/science.1060102)

[17] Fenberg, P.B., Posbic, K., & Hellberg, M.E. (2014). Historical and recent processes shaping the geographic range of a rocky intertidal gastropod: phylogeography, ecology, and habitat availability. *Ecology and Evolution*, *4*(16), 3244–3255. (https://doi.org/10.1002/ece3.1181)

[18] Jacobs, D.K., Haney, T.A., & Louie, K.D. (2004). Genes, diversity, and geologic process on the Pacific coast. *Annual Review of Earth and Planetary Sciences*, *32*(1), 601–652. (https://doi.org/10.1146/annurev.earth.32.092203.122436)

[19] Sanford, E. & Kelly M.W. (2011). Local adaptation in marine invertebrates. *Annual review of marine science, 3*(1), 509-535. (https://doi.org/10.1146/annurev-marine-120709-142756)

[20] Addicott, W.O. (1966). *Late Pleistocene marine paleoecology and zoogeography in central California*. US Government Printing Office. (https://doi.org/10.3133/pp523C)

[21] Roy, K., Valentine, J.W., Jablonski, D., & Kidwell, S.M. (1996). Scales of climatic variability and time averaging in Pleistocene biotas: implications for ecology and evolution. *Trends in Ecology & Evolution*, *11*(11), 458–463. (https://doi.org/10.1016/0169-5347(96)10054-9)

[22] Dawson, M.N. (2001). Phylogeography in coastal marine animals: a solution from California? *Journal of Biogeography, 28*(6), 723–736. (https://doi.org/10.1046/j.1365-2699.2001.00572.x)

[23] Marko, P. (1998). Historical allopatry and the biogeography of speciation in the prosobranch snail genus Nucella. *Evolution, 52*(3), 757-774. (https://doi.org/10.1111/j.1558-5646.1998.tb03700.x)

[24] McGovern, T.M., Keever, C.C., Saski, C.A., Hart, M.W., & Marko, P.B. (2010). Divergence genetic analysis reveals historical population genetic processes leading to contrasting phylogeographic patterns in co-distributed species. *Molecular Ecology, 19*(22), 5043-5060. (https://doi.org/10.1111/j.1365-294X.2010.04854.x)

[25] McGaughran, A., Liggins, L., Marske, K.A., Dawson, M.N., Schiebelhut, L.M., Lavery, S.D., Knowles, LL., Moritz, C. & Riginos, C. (2022). Comparative phylogeography in the genomic age: Opportunities and challenges. *Journal of Biogeography*, *49*(12), 2130–2144. (https://doi.org/10.1111/jbi.14481)

[26] Bringloe, T.T., Fort, A., Inaba, M., Sulpice, R., Ghriofa, C.N., Mols-Mortensen, A., Filbee-Dexter, K., Vieira, C., Kawai, H., Hanyuda, T., et al. (2022). Whole genome population structure of North Atlantic kelp confirms high-latitude glacial refugia. *Molecular Ecology*, *31*(24), 6473–6488. (https://doi.org/10.1111/mec.16714)

[27] Cheng, X. & Steinrücken, M. (2024). Population genomic scans for natural selection and demography. *Annual Review of Genetics, 58*, 319-339. (https://doi.org/10.1146/annurev-genet-111523-102651)

[28] Palmer, A.R. (1984). Prey selection by thaidid gastropods: some observational and experimental field tests of foraging models. *Oecologia*, *62*, 162-172. (https://doi.org/10.1007/BF00379009)

[29] Marko, P.B., Moran, A.L., Kolotuchina, N.K., & Zaslavskaya, N.I. (2014). Phylogenetics of the gastropod genus *Nucella* (Neogastropoda: Muricidae): species identities, timing of diversification and correlated patterns of life-history evolution. *Journal of Molluscan Studies, 80*(4), 341–353. (https://doi.org/10.1093/mollus/eyu024)

[30] Sanford, E., Roth, M.S., Johns, G.C., Wares, J.P., & Somero, G.N. (2003). Local selection and latitudinal variation in a marine predator-prey interactions. *Science, 300*(5622), 1135–1137. (https://doi.org/10.1126/science.1083437)

[31] Spight, T.M. (1975). On a snail's chances of becoming a year old. *Oikos*, 9-14. (https://doi.org/10.2307/3543270)

[32] Sanford, E. & Worth, D.J. (2010). Local adaptation along a continuous coastline: prey recruitment drives differentiation of a predatory snail. *Ecology, 91*(3), 891–901. (https://doi.org/10.1890/09-0536.1)

[33] Sanford, E. & Worth, D.J. (2009). Genetic differences among populations of a marine snail drive geographic variation in predation. *Ecology, 90*(11), 3108–3118. (https://doi.org/10.1890/08-2055.1)

[34] Longman, E.K. & Sanford, E. (2025). Biogeographic variation in mussel shell thickness and drilling predation on rocky shores. *Oecologia, 207*, 126. (https://doi.org/10.1007/s00442-025-05760-x)

[35] Neylan, I.P., Longman, E.K., Sanford, E., Stachowicz, J.J., & Sih, A. (2024). Long-term anti-predator learning and memory differ across populations and sexes in an intertidal snail. *Proceedings B, 291*(2032), 20240944. (https://doi.org/10.1098/rspb.2024.0944)

[36] Kuo, E.S., & Sanford, E. (2009). Geographic variation in the upper thermal limits of an intertidal snail: implications for climate envelope models. *Marine Ecology Progress Series*, *388*, 137–146. (https://doi.org/10.3354/meps08102)

[37] Schlötterer, C., Tobler, R., Kofler, R., & Nolte, V. (2014). Sequencing pools of individuals—mining genome-wide polymorphism data without big funding. *Nature Reviews Genetics*, *15*(11), 749–763. (https://doi.org/10.1038/nrg3803)

[38] Marko, P. (2005). An interspecific comparative analysis of character divergence between sympatric species. Evolution, 59(3), 554-564. (https://doi.org/10.1111/j.0014-3820.2005.tb01015.x)

[39] Bieler, R. (1992). Gastropod phylogeny and systematics. *Annual Review of Ecology and Systematics*, 311–338.

[40] Ye, C., Hill, C. M., Wu, S., Ruan, J., & Ma, Z. (2016). DBG2OLC: efficient assembly of large genomes using long erroneous reads of the third generation sequencing technologies. *Scientific Reports*, 6(1), 31900. (https://doi.org/10.1038/srep31900)

[41] Gurevich, A., Saveliev, V., Vyahhi, N., & Tesler, G. (2013). QUAST: quality assessment tool for genome assemblies. *Bioinformatics, 29*(8), 1072–1075. (https://doi.org/10.1093/bioinformatics/btt086)

[42] Manni, M., Berkeley, M.R., Seppey, M., Simão, F.A., Zdobnov, E.M. (2021). BUSCO update: novel and streamlined workflows along with broader and deeper phylogenetic

coverage for scoring of eukaryotic, prokaryotic, and viral genomes. *Molecular Biology and Evolution, 38*(10), 4647–4654. (https://doi.org/10.1093/molbev/msab199)

[43] Smit, A.F.A., Hubley, R., Green P. (2013-2015). RepeatMasker Open-4.0. http://www.repeatmasker.org

[44] Stanke, M., Keller, O., Gunduz, I., Hayes, A., Waack, S., & Morgenstern, B. (2006). AUGUSTUS: ab initio prediction of alternative transcripts. *Nucleic Acids Research, 34*, W435–W439. (https://doi.org/10.1093/nar/gkl200)

[45] Chen, S., Zhou, Y., Chen, Y., & Gu, J. (2018). Fastp: An ultra-fast all-in-one FASTQ processor. *Bioinformatics, 34*(17), i884–i890. (https://doi.org/10.1093/bioinformatics/bty560)

[46] Vasimuddin, M. Sanchit, M., Henge, L., Srinivas A. (2019). Efficient architecture-aware acceleration of BWA-MEM for multicore systems. *IEEE Parallel and Distributed Processing Symposiums (IPDPS)*. (https://doi:10.1109/IPDPS.2019.00041)

[47] Chen, Z., Baeza, J.A., Chen, C., Gonzalez, M.T., González, V.L., Greve, C., Kocot, K.M., Arbizu, P.M., Moles, J., Schell, T., et al. (2025). A genome-based phylogeny for Mollusca is concordant with fossils and morphology. *Science, 387*(6737), 1001–1007. (https://doi.org/10.1126/science.ads0215)

[48] Garrison, E., & Marth, G. (2012). Haplotype-based variant detection from short-read sequencing. *arXiv*, 1207.3907. (https://doi.org/10.48550/arXiv.1207.3907)

[49] Gautier, M., Vitalis, R., Flori, L., & Estoup, A. (2022). f-Statistic estimation and admixture graph construction with Pool-seq or allele count data using the R package poolfstat. *Molecular Ecology Resources, 22*, 1394–1416. (https://doi.org/10.1111/1755-0998.13557)

[50] Gautier, M. (2015). Genome-wide scan for adaptive divergence and association with population-specific covariates. *Genetics, 201*(4), 1555–1579. (https://doi.org/10.1534/genetics.115.181453)

[51] Ferretti, L., Ramos-Onsins, S.E., & Pérez-Enciso, M. (2013). Population genomics from pool sequencing. *Molecular ecology*, *22*(22), 5561–5576. (https://doi.org/10.1111/mec.12522)

[52] Jouganous, J., Long, W., Ragsdale, A.P., & Gravel, S. (2017). Inferring the joint demographic history of multiple populations: beyond the diffusion approximation. *Genetics*, *206*(3), 1549–1567. (https://doi.org/10.1534/genetics.117.200493)

[53] Nunez, J.C.B., Coronado-Zamora, M., Gautier, M., Kapun, M., Steindl, S., Ometto, L., Hoedjes, K.M., Beets, J., Wiberg, R.A.W., Mazzeo, G.R., et al. (2025). Footprints of worldwide adaptation in structured populations of *D. melanogaster* through the expanded DEST 2.0 genomic resource. *Molecular biology and evolution, 42*(8), msaf132. (https://doi.org/10.1093/molbev/msaf132)

[54] Keightley, P.D., Ness, R.W., Halligan, D.L., & Haddrill, P.R. (2014). Estimation of the spontaneous mutation rate per nucleotide site in a *Drosophila melanogaster* full-sib family. *Genetics, 196*(1), 313–320. (https://doi.org/10.1534/genetics.113.158758)

[55] Haller, B.C., & Messer, P.W. (2023). SLiM 4: multispecies eco-evolutionary modeling. *The American Naturalist*, *201*(5), E127–E139. (https://doi.org/10.1086/723601)

[56] Rohlf, F.J. (2015). The tps series of software. *Hystrix, 26*(1), 9–12. (https://doi.org/10.4404/hystrix-26.1-11264)

[57] Adams, D.C., Collyer, M., Kaliontzopoulou, A., & Baken, E. (2025). *Geomorph: Geometric morphometric analyses of 2D and 3D landmark data*. R package version 4.0.10. (https://doi.org/10.32614/CRAN.package.geomorph)

[58] Klingenberg, C.P. (2011). MorphoJ: an integrated software package for geometric morphometrics. *Molecular ecology resources*, *11*(2), 353-357. (https://doi.org/10.1111/j.1755-0998.2010.02924.x)

[59] Cingolani, P., Platts, A., Wang, L.L., Coon, M., Nguyen, T., Wang, L., Land, S.J., Lu, X., & Ruden, D.M. (2012). A program for annotating and predicting the effects of single nucleotide polymorphisms, SnpEff: SNPs in the genome of *Drosophila melanogaster* strain w1118; iso-2; iso-3. *fly*, *6*(2), 80–92. (https://doi.org/10.4161/fly.19695)

[60] McCartney, M.A., Auch, B., Kono, T., Mallez, S., Zhang, Y., Obille, A., Becker, A., Abrahante, J.E., Garbe, J., Badalamenti, J.P. et al. (2022). The genome of the zebra mussel, *Dreissena polymorpha*: a resource for comparative genomics, invasion genetics, and biocontrol. *G3*, *12*(2), jkab423. (https://doi.org/10.1093/g3journal/jkab423)

[61] Eastman, K.E., Pendleton, A.L., Shaikh, M.A., Suttiyut, T., Ogas, R., Tomko, P., Gavelis, G., Widhalm, J.R. & Wisecaver, J.H. (2023). A reference genome for the long-term kleptoplast-retaining sea slug *Elysia crispata* morphotype clarki. *G3: Genes, Genomes, Genetics*, *13*(12), jkad234. (https://doi.org/10.1093/g3journal/jkad234)

[62] Wares, J.P., & Cunningham, C.W. (2001). Phylogeography and historical ecology of the north Atlantic intertidal. *Evolution*, *55*(12), 2455–2469. (https://doi.org/10.1111/j.0014-3820.2001.tb00760.x)

[63] Anderson, E.C., Skaug, H.J., Barshis, D.J. (2014). Next-generation sequencing for molecular ecology: a caveat regarding pooled samples. *Molecular Ecology, 15*(5), 502-512. (https://doi.org/10.1111/mec.12609)

[64] Bergland, A.O., Tobler, R. González, J., Schmidt, P., & Petrov, D. (2016). Secondary contact and local adaptation contribute to genome-wide patterns of clinal variation in Drosophila melanogaster. *Molecular Ecology, 25*(5), 1157-1174. (https://doi.org/10.1371/journal.pgen.1006529)

[65] Spight, T.M. & Emlen, J. (1976). Clutch sizes of two marine snails with a changing food supply. *Ecology, 57*(6), 1162-1178. (https://doi.org/10.2307/1935042)

[66] Gravem, S.A., Bachhuber, S., Bignami, S., Chiachi, A.E., Field, L.C., Gaddam, R.N., Raimondi, P.T., & Menge, B.A. (2025). Biogeographic Patterns in Density, Recruitment, Body Size and Zonation of Rocky Intertidal Predators Suggest Increased Population Vulnerability Near Southern Range Limits. *Journal of Biogeography*, *52*(2), 257–273. (https://doi.org/10.1111/jbi.15029)

[67] Stephens, P.A., & Sutherland, W.J. (1999). Consequences of the Allee effect for behaviour, ecology and conservation. *Trends in ecology & evolution*, *14*(10), 401–405. (https://doi.org/10.1016/S0169-5347(99)01684-5)

[68] Smith, K.E., Aubin, M., Burrows, M.T., Filbee-Dexter, K., Hobday, A. J., Holbrook, N.J., King, N.G., Moore, P.J., Sen Gupta, A., Thomsen, M. et al. (2024). Global impacts of marine heatwaves on coastal foundation species. *Nature Communications*, *15*(1), 5052. (https://doi.org/10.1038/s41467-024-49307-9)

[69] Kadiwala, J., Hesketh, A., De Weerd, H., Ritch, H., & Shakur, R. (2025). The first genome Assembly of the Dogwhelk *Nucella lapillus*, a bioindicator species for the marine environment. *Scientific Data*, *12*(1), 1–8. (https://doi.org/10.1038/s41597-025-04764-9)

[70] Adema, C. M. (2021). Sticky problems: extraction of nucleic acids from molluscs. *Philosophical Transactions of the Royal Society B*, *376*(1825), 20200162. (https://doi.org/10.1098/rstb.2020.0162)

[71] Pascoe, P.L. Jha, A.N., & Dixon, D.R. (2004). Variation of karyotype composition and genome size in some muricid gastropods from the northern hemisphere. *Journal of Molluscan Studies, 70*(4), 389–398. (https://doi.org/10.1093/mollus/70.4.389)

[72] Chiba, S. (1993). Modern and historical evidence for natural hybridization between sympatric species in *Mandarina* (Pulmonata: Camaenidae). *Evolution, 47*(5), 1539-1556. (https://doi.org/10.1111/j.1558-5646.1993.tb02174.x)

[73] Crothers, J.H. (1984). Some observations on shell shape variation in Pacific *Nucella*. *Biological Journal of the Linnean Society, 21*(3), 259-281. (https://doi.org/10.1111/j.1095-8312.1984.tb00365.x)

[74] McLean, J.H. (2006). Hypothesis for the recognition of *Nucella analoga* (Forbes, 18520 in the northeastern Pacific. *Festivus, 38*, 17–21.

[75] Krug, P.J. (2009). Not my "type": larval dispersal dimorphisms and bet-hedging in Opisthobranch life histories. *The Biological Bulletin, 216*, 355-372.